Physics Letters A 416 (2021) 127652

Contents lists available at ScienceDirect

Physics Letters A

www.elsevier.com/locate/pla

Suppression of the nuclear forward scattering signal in $GdBaFe_2O_5$ and $PrBaFe_2O_5$

F. Lindroos [a], J.M.K. Slotte [a,b], J. Lindén [a,*], A.I. Chumakov [c], P. Karen [d]

[a] Physics, Faculty of Science and Engineering, Åbo Akademi University, FI-20500 Turku, Finland
[b] Accelerator Laboratory, Turku PET Centre, Åbo Akademi University, FI-20500 Turku, Finland
[c] ESRF, The European Synchrotron, 71 Avenue des Martyrs, CS40220, 38043 Grenoble Cedex 9, France
[d] Department of Chemistry, University of Oslo, P.O. Box 1033 Blindern, N-0315 Oslo, Norway

ARTICLE INFO

Article history:
Received 30 June 2021
Received in revised form 17 August 2021
Accepted 25 August 2021
Available online 3 September 2021
Communicated by L. Ghivelder

Keywords:
Mössbauer spectroscopy
Nuclear forward scattering
Double perovskites
Verwey transition
Intermittent suppression of coherent decay-channel
Valence mixing

ABSTRACT

Antiferromagnetic double-cell perovskites $GdBaFe_2O_{5.004}$ and $PrBaFe_2O_{5.001}$ were studied with 14.4 keV ^{57}Fe nuclear forward scattering (NFS). Both have charge- and orbital-ordered iron below a Verwey transition temperature T_V and valence-mixed iron above a second transition at a higher T_p. At intermediate temperatures $T_V < T < T_p$, only a partial charge separation remains and more than 75% of the NFS signal is suppressed. The breakdown of the coherent signal is due to broadening of the nuclear resonance by local disorder of the two partially charge-separated iron species at the single crystallographic Fe site.

1. Introduction

Transition-metal double-cell perovskites RAM_2O_5, with A = Ba or Sr, M = Co, Mn or Fe, and R a rare-earth element, have attracted considerable interest, where the Co-variant is a material potentially interesting for solid-oxide fuel cells [1–4]. Both the Mn and Co variants order their ionic charges at sufficiently low temperatures [5,6]. Antiferromagnetic iron-based double-cell perovskites of the type $RBaFe_2O_5$, with R = Nd, Sm, Gd, Eu, Tb, Dy, Ho, or Y are charge ordered (CO) into Fe^{3+} and into Fe^{2+} of ordered doubly-occupied d_{xz} orbitals below T_V of the first-order Verwey transition [7–14]. Above a second-order transition at a higher temperature T_p, valence-mixed (VM) $Fe^{2.5+}$ forms. The intermediate (IM) range between these two transitions is dominated by partially mixed $Fe^{2+\delta}$ and $Fe^{3-\delta}$ lacking long-range order [14]. For $RBaFe_2O_5$ of small Y^{3+}/Ho^{3+} to Sm^{3+} ions, both transitions are sharp with only minor overlap between the temperature ranges dominated by the CO, IM and VM iron species. For the large $R = Nd^{3+}$, the overlap increases [7–9], and the charge-ordered structure distorts [15]. The temperature evolution of the Fe species has previously been investigated by conventional, energy-domain (ED), ^{57}Fe Mössbauer spectroscopy [8,11,9,7,14]. For $PrBaFe_2O_5$ of the largest compatible R[16], the overlap of the Fe species further increases, and this calls for high-resolution data.

Mössbauer spectra can also be measured in the time domain by nuclear forward scattering (NFS) [17]. In this method, the information is gathered from the time-dependent decay of the collectively excited nuclear states, instead of the absorption by individual nuclei as in ED Mössbauer spectroscopy. Due to the collective nature of the excitation in NFS, the method is sensitive to the coherence of the excited states of the ^{57}Fe nuclei as well as to any fluctuations occurring on the ∼10 ns scale. The high brilliance of the synchrotron source and the very high signal-to-noise ratio facilitates quick data collection. In this paper, we report an unexpected observation of a strong decrease in the NFS count rate in the IM temperature range in $GdBaFe_2O_5$ (Gd112) and $PrBaFe_2O_5$ (Pr112), which is further enhanced by an external magnetic field.

2. Experimental

The samples were synthesized from amorphous precursors as described in Ref. [16]. One Pr112 pellet of ∼2 g mass was then annealed for 72 hours at 840 °C and quenched from $\log(p_{O_2}/\text{bar}) = -20.73$ obtained in a flow of 99.9% hydrogen wetted in H_2O

* Corresponding author.
E-mail address: johan.linden@abo.fi (J. Lindén).

https://doi.org/10.1016/j.physleta.2021.127652

at 17.7 °C. Oxygen-content analysis [16] yielded $PrBaFe_2O_{5.001(2)}$. The Gd112 precursor was calcined [880 °C, 25 h, $\log(p_{O_2}/\text{bar}) = -15.56(3)$, Ar/H_2 = 145(4)], pressed into pellets, sintered [1040 °C, 30 h, $\log(p_{O_2}/\text{bar}) = -14.54(2)$, Ar/H_2 = 19.7(5)] and densified [1000 °C, 72 h, $\log(p_{O_2}/\text{bar}) = -15.60$, Ar/H_2 = 11.5]. One pellet was then annealed for 73 hours at 1000 °C and $\log(p_{O_2}/\text{bar}) = -15.80$ reached in a flow of 9.8% hydrogen in argon (mixed analyzed gas of 5N purity, AGA) wetted in H_2O at 17.7 °C, then quenched to $GdBaFe_2O_{5.004(2)}$.

The absorber disks (1 mm height, 3 mm diameter) of Gd112 and Pr112 for the NFS measurements were punched from larger disks made of epoxy glue with 35 (37) mg/cm^2 of powder for Gd112 (Pr112). Experiments were performed with radiation of energy 14.412 keV and a bandwidth of 0.8 meV at the Nuclear Resonance Beamline ID18 [18] of the European Synchrotron Radiation Facility, operating in a 16-bunch mode with 176 ns between the bunches and an average current of 89 mA. The forward-scattered gamma quanta were detected by a stack of four fast-gated silicon avalanche photodiodes inclined 30° to increase efficiency. The count rate of the forward-scattered signal was recorded immediately after every optimization routine of the monochromator and corrected for small variations in the intensity of the incident beam.

15 spectra of Gd112 and 20 of Pr112 across the CO, IM, and VM states were collected for ∼30 min (Gd112) and ∼45 min (Pr112) at temperatures between 5 and 317 K controlled by the cryomagnetic system of the beamline. Additional two measurements at 247 and 283 K for Gd112 and two at 246 and 317 K for Pr112 were done in an external magnetic field of 4.0 T applied in a direction parallel with the beam. The MOTIF program [19] was used to fit each spectrum with the actually present CO, IM, and VM iron species (pairs of Fe ions in each of these three states) as spectral components. Two additional components of small and fixed-equal relative intensity were included, pertaining to paramagnetic iron ions that have earlier [14] been identified as antiphase boundaries. Each component was fitted with individual additional Lorentzian broadening, relative intensity, isomer shift, quadrupole coupling constant, and magnetic field (except for paramagnetic components in spectra with no external field). For comparison with these NFS results, absorbers were made from the same two samples and measured with conventional ED Mössbauer spectroscopy with a 4-months old ^{57}Co Mössbauer source (25 mCi, Ritverc GmbH).

3. Results and discussion

NFS spectra are not as straightforward to interpret as ED spectra. While ED spectra are a sum of individual components Fe^{2+}, Fe^{3+}, $Fe^{2+\delta}$, $Fe^{3-\delta}$ and $Fe^{2.5+}$, NFS spectra appear as quantum beats originating from an interference of sub-waves scattered by various hyperfine transitions of a collective excitation of all Fe atoms in the sample. It is somewhat similar to studying an acoustic signal (in time domain) versus observing its Fourier spectrum. Nevertheless, both yield the same hyperfine parameters. The advantage of NFS is the short data acquisition time and high signal-to-noise ratio.

NFS spectra typical of the CO, IM, and VM states are illustrated in Fig. 1 for Gd112 and in Fig. 2 for Pr112. The fittings show that the CO state is dominated by Fe species with hyperfine parameter values compatible with high-spin charge-ordered Fe^{3+} and Fe^{2+} (the latter orbital ordered), the IM state is dominated by partially valence-mixed $Fe^{2+\delta}$ and $Fe^{3-\delta}$, and the VM state is dominated by $Fe^{2.5+}$. The relative portions of the CO, IM, and VM atoms obtained from the fittings are plotted in Figs. 3 and 4. The results for Gd112 in Fig. 3 agree with values obtained by ED measurements for $GdBaFe_2O_5$ [9] and the similar $YBaFe_2O_5$ [14]. Due to the large ionic radius of Pr, the results for Pr112 in Fig. 4 exhibit weaker charge separation and larger overlap between the three groups of

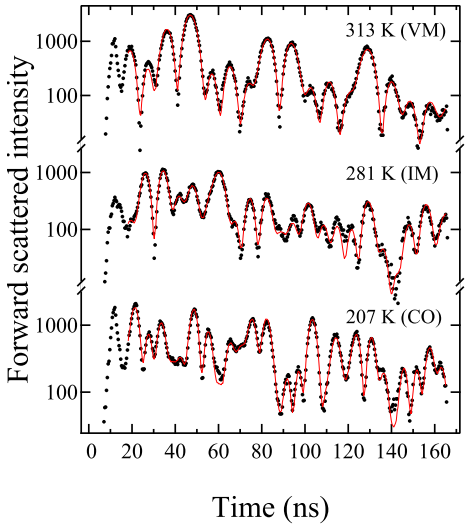

Fig. 1. Fitted ^{57}Fe NFS Mössbauer spectra of Gd112 recorded at indicated temperatures below $T_V \approx 269$ K, between T_V and T_p, and above $T_p \approx 306$ K.

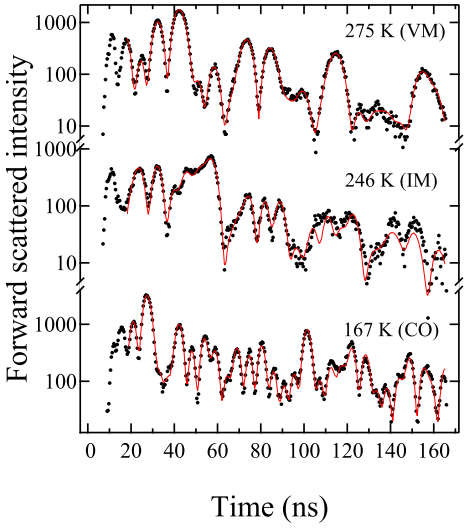

Fig. 2. Fitted ^{57}Fe NFS Mössbauer spectra of Pr112 recorded at indicated temperatures below $T_V \approx 207$ K, between T_V and T_p, and above $T_p \approx 266$ K.

valence states than in Gd112; similar to $NdBaFe_2O_5$ [7], the closest compound in the $RBaFe_2O_5$ series with reported ED data.

The count rates for the NFS measurements, which are the numbers of photons per time emitted in the forward direction following the initial synchrotron pulse, are plotted in Figs. 5 and 6. These count rates strongly decrease in the IM temperature range for both Gd112 and Pr112. This can also be seen in Figs. 1 and 2, where the IM spectra have lower intensity than the CO and VM spectra, despite being measured for the same time. For thin samples, the count rates in NFS measurements scale in general with the recoil-free fraction f of absorption as f^2, while the scaling is linear with f in ED measurements. However, the temperature evolution of the isomer shift and absorption area in ED Mössbauer spectra [14] do not show any corresponding decrease in Debye temperature in the IM range. Instead, the Debye temperature increases upon heating past T_V and remains constant over the rest of the measured temperature range. Therefore, the temperature evolution of the recoil-free fraction is only expected to cause a monotonous decrease in NFS count rate over the measured temperature range; it cannot cause the observed decrease in the IM region. Other mechanisms must be invoked.

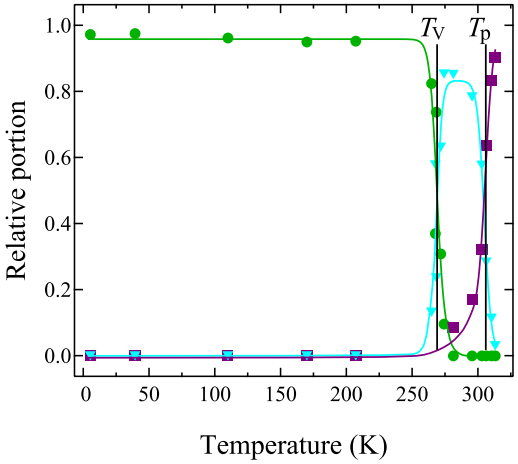

Fig. 3. The relative portions of the CO (green bullets), IM (cyan triangles), and VM (magenta squares) states vs. temperature for sample Gd112, obtained by fitting NFS data. Lines are drawn as guides for eye. (For interpretation of the colors in the figure(s), the reader is referred to the web version of this article.)

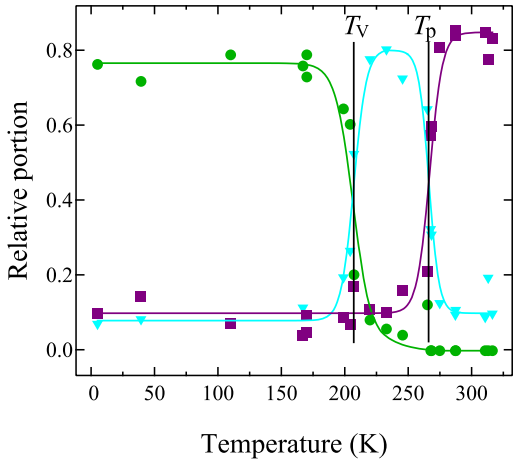

Fig. 4. The relative portions of the CO (green bullets), IM (cyan triangles), and VM (magenta squares) states vs. temperature for sample Pr112, obtained by fitting NFS data. Lines are drawn as guides for eye.

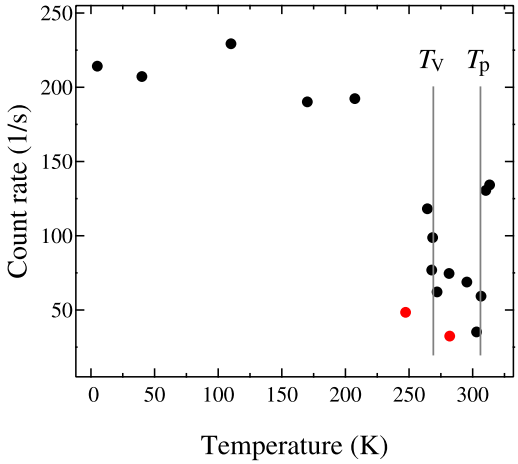

Fig. 5. Count rate for the NFS measurements of sample Gd112 (black bullets) decreases in the IM range between T_V and T_p. The application of an external magnetic field of 4.0 T also suppresses the count rate (red bullets).

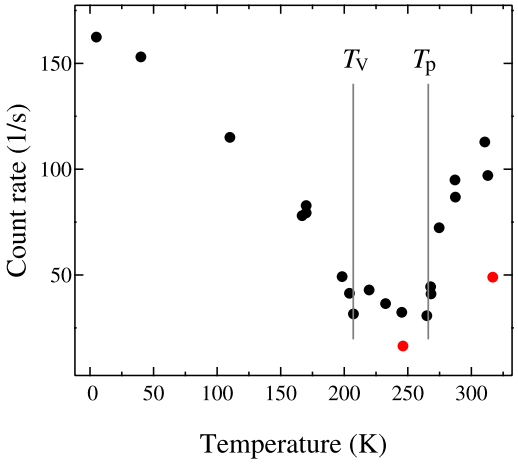

Fig. 6. Count rate for the NFS measurements of sample Pr112 (black bullets) decreases in the IM range between T_V and T_p. The application of an external magnetic field of 4.0 T also suppresses the count rate (red bullets).

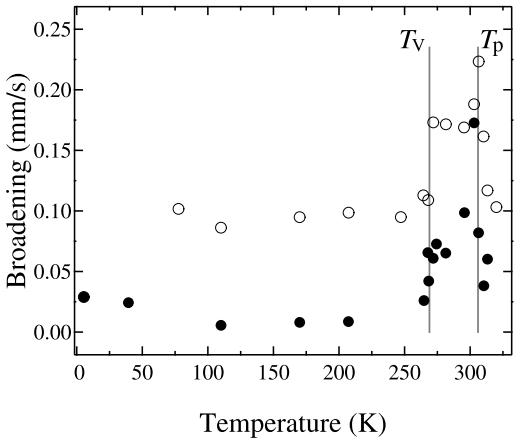

Fig. 7. Average Lorentzian broadening obtained by fitting the NFS (bullets) and ED (circles) spectra of sample Gd112.

The NFS signal is caused by coherent decays of collective excitations of all ^{57}Fe atoms. Suppression of the coherent decay-channel manifested as a decrease of the count rate in the forward direction can be associated with broadening of resonance lines that suppresses the coherent signal [20]. Such a broadening can arise if the internal magnetic field perceived by the Mössbauer nuclei, or their electric field gradients and isomer shifts, widen into distributions. Indeed, fitting the NFS data from the IM range (Figs. 7 and 8) suggests a substantial Lorentz broadening. Measurements of the same samples by ED Mössbauer spectroscopy also show a broadening of the average linewidth in the IM range, Figs. 7 and 8, but no decrease in absorption. There is a clear correlation between the broadening and the decrease in the NFS count rate in Figs. 5 and 6. The larger overlap of the valence states in Pr112 also correlates with the more gradual decrease in the NFS count rate, not so strictly confined to the IM range as for Gd112.

A similar effect is seen when an external magnetic field is applied to these antiferromagnetic samples. The four NFS spectra collected under applied field of 4.0 T show an additional decrease in the count rate (Figs. 5 and 6). The reason is the random orientation of the applied field with respect to the internal magnetic field seen by the nuclei of each antiferromagnetic iron specie present in various magnetic domains of all crystallites in the grains of the powder absorber. Due to the random angle between the external and internal magnetic field, the summing of the fields leads to broadening of the resonance lines. That suppresses the NFS sig-

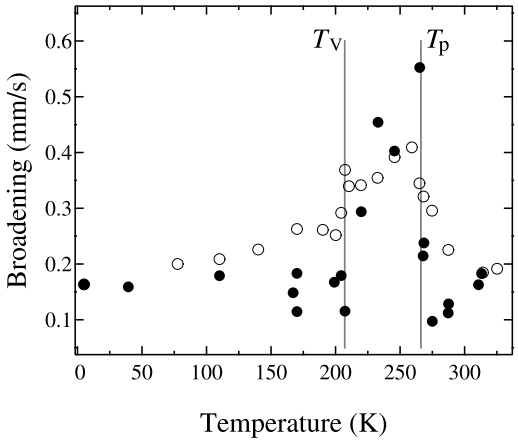

Fig. 8. Average Lorentzian broadening obtained by fitting the NFS (bullets) and ED (circles) spectra of sample Pr112.

nal of all valence states in all three ranges, CO, IM, and VM, at all temperatures.

4. Conclusions

The exclusive suppression of the NFS coherent decay-channel in the IM temperature range of these double-cell perovskites also stems from broadened distribution of the hyperfine fields; a distribution caused by the weak charge separation of Fe atoms. That charge separation is a local disorder of incompletely mixed valences that remain after the long-range charge-ordered iron species have largely mixed upon heating past T_V, replacing the cooperative d_{xz}-orbital order that kept them ready to mix. In the IM range, diffraction experiments detect one symmetry-equivalent Fe atom; no long-range order of its remaining higher- and lower-charge versions. They appear all equal, but they are not because they still have to mix more completely at T_p. Each unit cell has Fe atoms with slightly different neighborhoods of oxygens and somewhat different charge at Fe. As each Fe nucleus perceives slightly different hyperfine fields, the originally sharp distribution of the CO range widens in the IM range into a broad distribution of hyperfine-field magnitudes and orientations. That suppresses the coherent decay-channel. Neither does diffraction see the more complete mixing at T_p, which is registered by differential scanning calorimetry (Pr112 [16], Gd112 [12]). The rare sequence of order, disorder, order at the crystal-structure sites accommodating the gradually mixing iron-valence species makes these perovskites a unique example of an intermittent suppression of the NFS signal as a function of temperature.

CRediT authorship contribution statement

Johan Lindén: Supervision, Conceptualization, Methodology, Software, Original draft preparation Project Administration. Fredrik Lindroos: Investigation, Formal analysis, Original draft preparation. Joakim Slotte: investigation. Pavel Karen: Resources, Writing-Reviewing and Editing. A. Chumakov: Supervision, Resources, Reviewing and Editing.

Declaration of competing interest

The authors declare that they have no known competing financial interests or personal relationships that could have appeared to influence the work reported in this paper.

Acknowledgements

We acknowledge the European Synchrotron Radiation Facility for provision of synchrotron radiation facilities and we would like to thank Dr D. Bessas for assistance in using beamline ID18. F.L. acknowledges financial support from Åbo Akademi University and its Doctoral Network in Materials Research. F.L., J.L. and J.S. acknowledge financial support from the Waldemar von Frenckell Foundation. F.L. and J.S. acknowledge financial support from the Swedish cultural foundation of Finland.

References

[1] A. Tarancón, S.J. Skinner, R.J. Chater, F. Hernández-Ramírez, J.A. Killner, J. Mater. Chem. 17 (2007) 3175–3181.
[2] I. Kim, M. Cho, ACS Omega 4 (2019) 10960.
[3] S. Roy, I.S. Dubenko, M. Khan, E.N. Condon, J. Craig, N. Ali, W. Liu, B.S. Mitchell, Phys. Rev. B 71 (2005) 024419.
[4] E.L. Rautama, M. Karppinen, J. Solid State Chem. 183 (2010) 1102–1107.
[5] F. Millange, V. Caignaert, D. Domengès, B. Raveau, Chem. Mater. 10 (1998) 1974–1983.
[6] T. Vogt, P.M. Woodward, P. Karen, B.A. Hunter, P. Henning, A.R. Moodenbaugh, Phys. Rev. Lett. 84 (2000) 2969–2972.
[7] J. Lindén, P. Karen, J. Phys. Condens. Matter 24 (2012) 376002.
[8] J. Lindén, P. Karen, A. Kjekshus, J. Miettinen, T. Pietari, M. Karppinen, Phys. Rev. B 60 (1999) 15251–15260.
[9] J. Lindén, F. Lindroos, P. Karen, Hyperfine Interact. 226 (2014) 229–239.
[10] P. Karen, K. Gustafsson, J. Lindén, J. Solid State Chem. 180 (2007) 148–157.
[11] P. Karen, P.M. Woodward, J. Lindén, T. Vogt, A. Studer, P. Fischer, Phys. Rev. B 64 (2001) 214405.
[12] P. Karen, J. Solid State Chem. 177 (2004) 281–292.
[13] P.M. Woodward, E. Suard, P. Karen, J. Am. Chem. Soc. 125 (2003) 8889–8899.
[14] J. Lindén, F. Lindroos, P. Karen, J. Solid State Chem. 252 (2017) 119–128.
[15] P. Karen, P.M. Woodward, P.N. Santhosh, T. Vogt, P.W. Stephens, S. Pagola, J. Solid State Chem. 167 (2002) 480–493.
[16] P. Karen, J. Solid State Chem. 299 (2021) 122147.
[17] E. Gerdau, H. DeWaard, Hyperfine Interact. 123 (1999) 0–0.
[18] R. Rüffer, A.I. Chumakov, Hyperfine Interact. 97–98 (1996) 589–604.
[19] Y.V. Shvyd'ko, Hyperfine Interact. 125 (2000) 173–188.
[20] G. Smirnov, Hyperfine Interact. 123 (1999) 31–77.